

Supplementary Information

Selective Chemical Vaporization of Exogenous Tellurium for Characterizing the Time- Dependent Biodistribution and Dissolution of Quantum Dots in Living Rats

Cheng-Kuan Su, Ting-Yu Cheng, and Yuh-Chang Sun*

Department of Biomedical Engineering and Environmental Sciences, National Tsing-Hua
University, Hsinchu, 30013, Taiwan.

* To whom correspondence should be addressed.

Fax: +886-3-5723883, Tel.: +886-3-5727309

e-mail: ycsun@mx.nthu.edu.tw

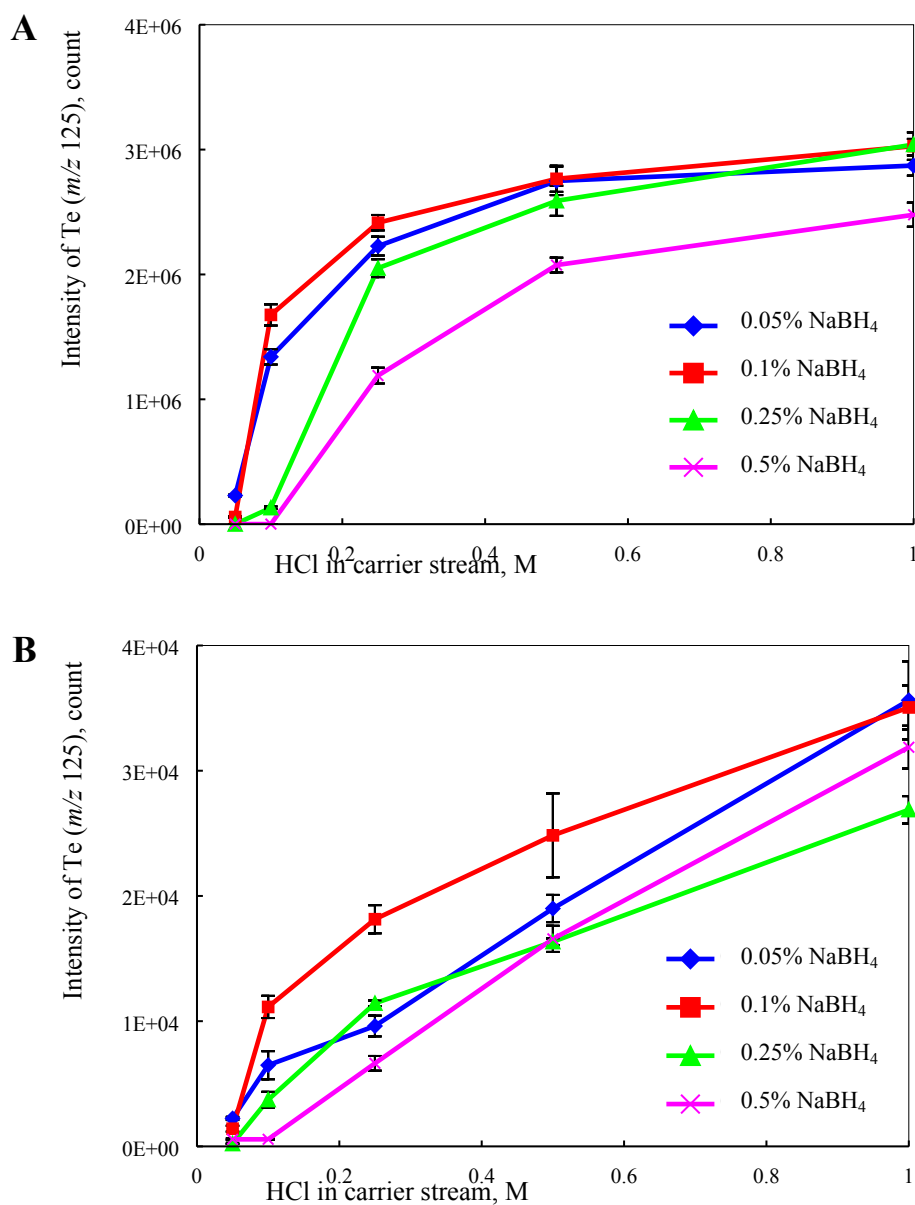


Fig. S2. Signal intensities of TeO_3^{2-} (A) and QD705 (B) plotted with respect to the concentrations of NaBH_4 and HCl in carrier stream for our established chemical VG scheme. The concentrations of the both Te species were $1 \mu\text{g Te L}^{-1}$. Error bars represent standard deviations ($n = 5$).

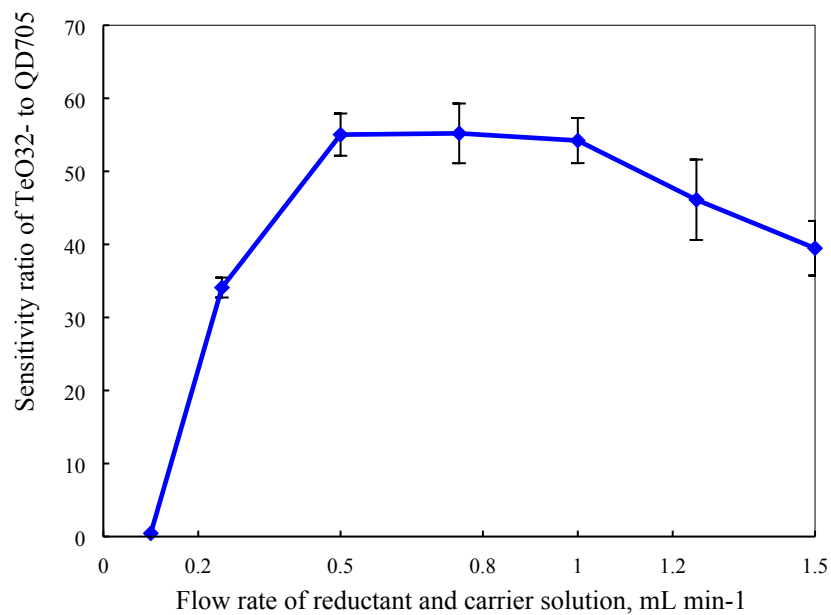


Fig. S3. Intensity ratios of TeO_3^{2-} to QD705 plotted with respect to the flow rates of NaBH_4 and carrier solution for the established chemical VG scheme. Values are expressed as the ratio of the signal intensity of TeO_3^{2-} to that of QD705 under the condition of an equal concentration ($1 \mu\text{g Te L}^{-1}$) of the two species. Error bars represent standard deviations ($n = 5$).

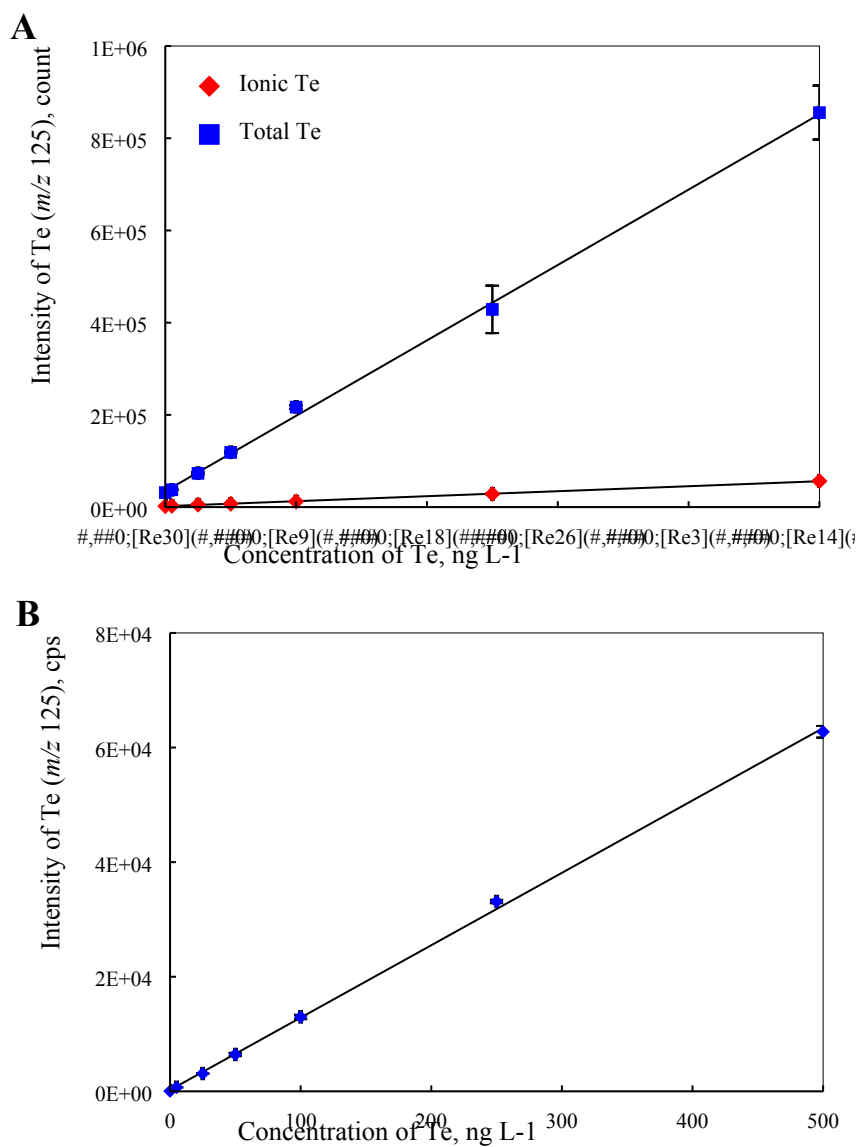


Fig. S4. Calibration curves of the released and total Te established by our chemical VG method (A), and that of the only total Te established by routine ICP-MS analysis method (B).

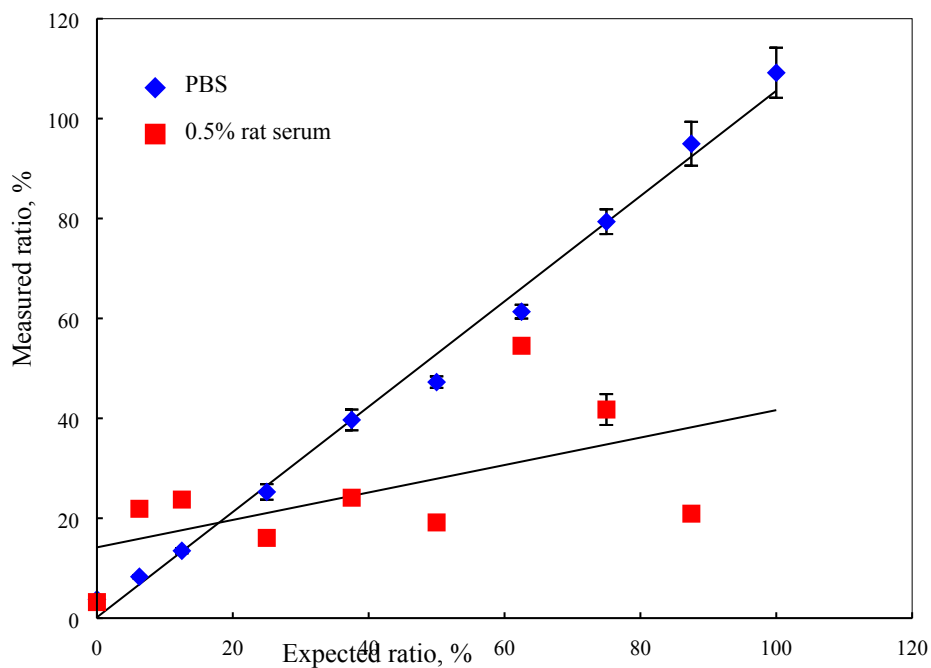


Fig. S5. Correlation between the expected and experimentally measured ratios of Se_T (released Se)/ Se_{total} (total Se) in PBS and rat serum samples. Experiments were conducted using the conditions as that for Te vaporization. The totally spiked Se concentrations of the two species (SeO_3^{2-} and QD705) were fixed at $7.2 \mu g L^{-1}$. Error bars represent standard deviations ($n = 5$).

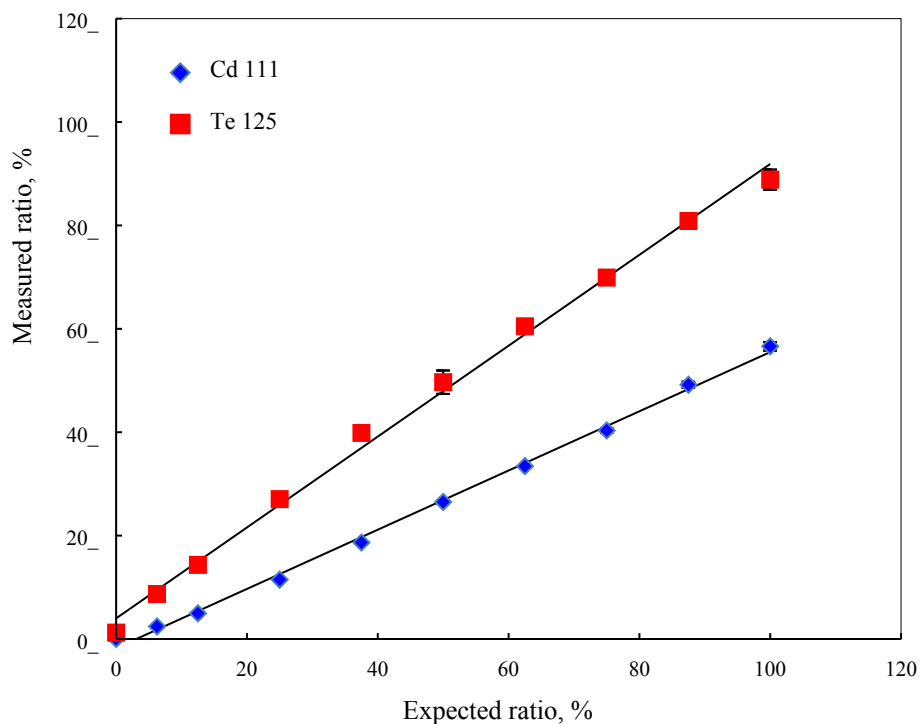


Fig. S6. Correlation between the expected and experimentally measured ratios of Te_r/Te_{total} and Cd^{2+}/Cd_{total} by centrifugal filtration method. The totally spiked Te and Cd (Cd^{2+} and QD705) concentrations were fixed at 0.5 and 29.1 $\mu g L^{-1}$, respectively. Error bars represent standard deviations ($n = 5$).

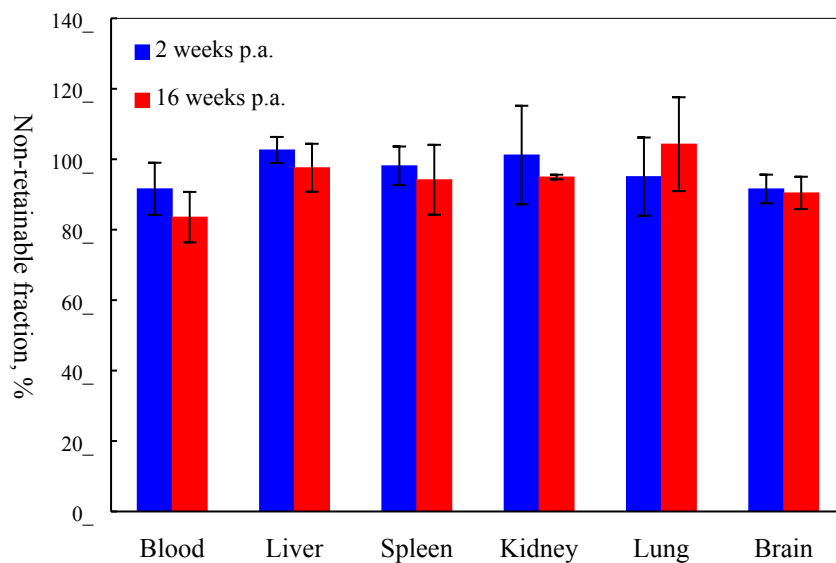


Fig. S7. The C₁₈ non-retainable fractions of Te species in solubilized rat organs and tissues 2 and 16 weeks post-administration. As for our developed sample pretreatment procedure, each rat sample was solubilized, diluted, and then passed through the C₁₈ cartridge before the hydride generation scheme. The non-retainable fractions were defined by the Te signal intensities (m/z 125) of the rat samples passed through C₁₈ cartridge to that without C₁₈ pretreatment.

Table S1. QD705 Biodistribution based on total Te concentrations determine by HG-ICP-MS method and routine ICP-MS analysis method

	2 weeks post-administration		16 weeks post-administration	
	Te _{total} determined by HG-ICP-MS, $\mu\text{g L}^{-1}$	Te _{total} determined by ICP-MS, $\mu\text{g L}^{-1}$	Te _{total} determined by HG-ICP-MS, $\mu\text{g L}^{-1}$	Te _{total} determined by ICP-MS, $\mu\text{g L}^{-1}$
Blood	4.8 ± 1.2	4.3 ± 1.2	1.2 ± 0.2*	1.9 ± 0.3
Liver	8.3 ± 1.2	7.8 ± 0.9	2.1 ± 0.3	2.3 ± 0.2
Spleen	10.3 ± 1.9	10.0 ± 2.6	2.0 ± 0.1	2.3 ± 0.3
Kidney	6.9 ± 1.9	6.2 ± 1.1	2.0 ± 0.4	1.7 ± 0.3
Lung	3.8 ± 0.9	3.9 ± 0.6	1.4 ± 0.3	1.3 ± 0.3
Brain	1.1 ± 0.9	1.1 ± 0.2	0.7 ± 0.4	0.7 ± 0.4

*The value determined by HG-ICP-MS method was significantly different to that by routine ICP-MS analysis method.